

The Curious Case of Nonverbal Abstract Reasoning with Multi-Modal Large Language Models

Kian Ahrabian* Zhivar Sourati* Kexuan Sun*
Jiarui Zhang Yifan Jiang Fred Morstatter Jay Pujara
Information Sciences Institute, Marina del Ray, USA
University of Southern California, Los Angeles, USA

{ahrabian, souratih, kexuansu, jzhang37, yifjia}@usc.edu, {fredmors, jpujara}@isi.edu

Abstract

While large language models (LLMs) are still being adopted to new domains and utilized in novel applications, we are experiencing an influx of the new generation of foundation models, namely multi-modal large language models (MLLMs). These models integrate verbal and visual information, opening new possibilities to demonstrate more complex reasoning abilities at the intersection of the two modalities. However, despite the revolutionizing prospect of MLLMs, our understanding of their reasoning abilities is limited. In this study, we assess the nonverbal abstract reasoning abilities of open-source and closed-source MLLMs using variations of Raven’s Progressive Matrices. Our experiments reveal the challenging nature of such problems for MLLMs while showcasing the immense gap between open-source and closed-source models. We also uncover critical shortcomings of visual and textual perceptions, subjecting the models to low-performance ceilings. Finally, to improve MLLMs’ performance, we experiment with different methods, such as Chain-of-Thought prompting, leading to a significant (up to 100%) boost in performance. Our code and datasets are available at [here](#).

1 Introduction

Foundation models — mostly large language models (LLMs) and large vision models (LVMs) — have revolutionized the field of artificial intelligence, demonstrating zero-shot (Radford et al., 2019; Wang et al., 2023a) and few-shot (*i.e.*, in-context) learning abilities (Brown et al., 2020; Zhang et al., 2023b) that perform on-par or even surpass humans in some tasks (Webb et al., 2023). These tasks cover both dimensions of general intelligence: crystallized intelligence focusing on retrieving knowledge from memory (Hartmann et al., 2023) and fluid intelligence involving novel and abstract reasoning (Cattell, 1987). Following these

* Authors contributed equally.

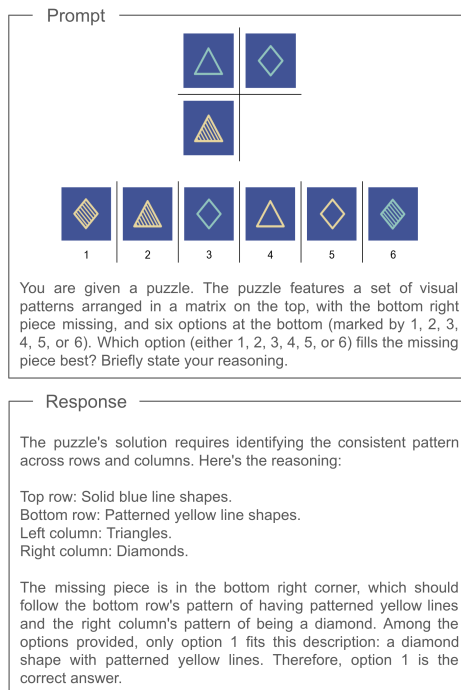


Figure 1: An example of model’s prediction on a sample from the IQ50 dataset. Given a prompt with a visual puzzle (*top*), the model generates a response that includes its reasoning and the chosen option.

advancements, there has been a recent surge in the development of a new generation of foundation models, namely, multi-modal large language models (MLLMs). These models can process visual and textual cues (OpenAI, 2023; Zhao et al., 2023; Huang et al., 2023), paving the way for solving far more complex tasks concerning both modalities.

Nonverbal abstract reasoning is a family of tasks involving both modalities. It has been studied extensively for measuring fluid intelligence (Sha-keel et al., 2017), in which reasoners need to demonstrate strong visual perception and high-level explicit reasoning abilities to solve these tasks. Prior studies have explored the performance of LVMs (Zhuo and Kankanhalli, 2020)

and LLMs (Hu et al., 2023; Webb et al., 2023) on transformed versions of these tasks in an unimodal setting. However, theoretical and empirical evidence exists for the benefits of the interplay between verbal and visual perceptions (Vyshedskiy, 2019; Winawer et al., 2007; Vygotsky, 1962), suggesting that visual perception helps us better understand our surroundings, while language helps us symbolize and facilitate reasoning through notions such as self-talk (Berk, 1994).

Inspired by prior works (Vygotsky, 1962; Lupyan, 2012; Nam et al., 2017; Colas et al., 2021) that have explored the fusion of visual and verbal cues and their effect on cognition and reasoning abilities, and considering the opportunity of experimenting with both modalities in MLLMs, in this study, we strive to answer the following research question: **Do MLLMs demonstrate faithful non-verbal abstract reasoning abilities?**

Our contributions are as follows:

1. We evaluate the nonverbal abstract reasoning abilities of 24 open-source and closed-source MLLMs under three Raven’s Progressive Matrices (RPM) (Raven, 2003) benchmarks (See Figure 1 for an example);
2. We evaluate MLLMs’ textual and visual capabilities in pseudo-isolated settings that mitigate cross-modality error contamination, providing insights into their performance ceiling.
3. We evaluate MLLMs’ zero-shot and few-shot abilities, drawing a more accurate picture of the alignment between their verbal and visual perceptions;

All in all, we observe that while open-source MLLMs perform poorly on nonverbal abstract reasoning tasks, closed-source models such as GPT-4V (OpenAI, 2023) showcase non-trivial abilities (See Section 4). Moreover, we discover critical shortcomings in both visual and verbal capabilities across open-source and closed-source models, partially explaining the observed poor performances (See Section 5). Finally, we find closed-source models’ textual and visual perceptions to be relatively aligned, allowing us to improve their performance significantly by providing guided prompts and in-context demonstrations (See Section 6).

2 Related Work

Foundation Models’ Reasoning Abilities. With the advancements of large pre-trained (*i.e.*, foun-

dation) models (Vaswani et al., 2017; Dosovitskiy et al., 2020), researchers have extensively evaluated their reasoning abilities (Bubeck et al., 2023). These evaluations go beyond simple knowledge retrieval (Zhu et al., 2023b; Hartmann et al., 2023), focusing on tasks that require novelty and abstractions built on models’ knowledge (Rytting and Wingate, 2021), covering visual (Zhuo and Kankanhalli, 2020; Jahrens and Martinetz, 2020; Barrett et al., 2018) and textual (Webb et al., 2023; Hu et al., 2023; Lu et al., 2022; Hill et al., 2019; Wei et al., 2022) dimensions.

MLLMs. Wide-spread utilization of foundation models and their role as general-purpose interfaces to different modalities (Hao et al., 2022) have led to the development of MLLMs (Li et al., 2022; Chen et al., 2022; Alayrac et al., 2022; Li et al., 2023a; Wang et al., 2022; Zhu et al., 2023a) that can generate text conditioned on the combination of different modalities, demonstrating zero-shot (Li et al., 2022), few-shot (Alayrac et al., 2022; Zhao et al., 2023), and chain-of-thought abilities (Huang et al., 2023). To better understand their range of abilities, prior studies have evaluated MLLMs for geometric reasoning (Kazemi et al., 2023), text recognition (Liu et al., 2023b), mathematical reasoning (Lu et al., 2024), college-level deliberate reasoning (Yue et al., 2023), and open-ended reasoning (Han et al., 2023) abilities. Most similar to our study are the works of Qi et al. (2023) and Mitchell et al. (2023), evaluating the abstract reasoning abilities of MLLMs; however, their evaluation is either limited to a few examples or lack the rigor to provide an in-depth understanding. In this study, we bridge the gap in the literature by conducting extensive experiments that produce comprehensive insights into MLLMs’ abstract reasoning abilities.

3 Experimental Setup

3.1 Datasets

IQ50. Introduced by Huang et al. (2023), IQ50 is a nonverbal reasoning benchmark containing 50 visual puzzles crawled from the internet. Given a set of images arranged in a matrix or a sequence, the goal is to predict the missing piece of the puzzle from six given options. To conduct our extensive experiments, we augment each puzzle with textual description and hint annotations to explore the interplay between textual cues and visual perceptions.

RAVEN. Introduced by Zhang et al. (2019), RAVEN is a relational and visual reasoning dataset containing 70,000 synthetic samples in seven categories (each 10,000). Each instance is created following a sampled rule and contains a 3x3 matrix of images (with the bottom right piece missing) and eight options, with a goal similar to IQ50. To reduce the computational costs, we randomly sample 500 examples from each category (3,500 in total) to create RAVEN-S.

CCSE. We collected 175 visual abstractions and reasoning problems from the China Civil Service Examination (CCSE), each containing a matrix or a sequence of images with four options. This newly curated dataset serves as a challenging benchmark across various reasoning patterns. See Appendix E for more details.

3.2 Models

Pre-Trained. The first set of models that we utilize in our experiments are state-of-the-art pre-trained MLLMs. Specifically, we chose the following models due to their popularity and accessibility: 1) BLIP-2 (Li et al., 2023a), 2) Fuyu (Bavishi et al., 2023), 3) IDEFICS (Laurençon et al., 2023), and 4) Qwen-VL (Bai et al., 2023). Note that all these models, except for the BLIP-2 family, have undergone a multi-task pre-training procedure, presumably allowing them to have zero-shot abilities on a wide range of tasks (See Appendix B).

Instruction-Tuned. The second set of models that we use in our experiments are state-of-the-art instruction-tuned MLLMs. Specifically, we chose the following models with similar criteria as pre-trained MLLMs: 1) InstructBLIP (Dai et al., 2023), 2) MMICL (Zhao et al., 2023), 3) LLaVA (Liu et al., 2023a) 4) IDEFICS (Laurençon et al., 2023), 5) Qwen-VL (Bai et al., 2023), 6) GPT-4V (OpenAI, 2023), and 7) Gemini (Google, 2023).

Heuristics. Since most of our samples follow similar spatial patterns and the task is to fill the missing image with the best candidate, we can write the expected representation of the target image as a function of the provided query images. To this end, we first compute the target image’s expected representation as

$$r = \sum_{q \in Q} \alpha_q R(q), \quad (1)$$

where R is a function mapping images to vector representations, Q is the set of all query images,

and $\alpha_q \in \mathbb{R}$ is the weight of image q . For simplicity, we only consider linear combinations. Then, we select the candidate p that has the highest similarity to r as our prediction:

$$p = \operatorname{argmax}_{c \in C} S(r, R(c)), \quad (2)$$

where C is the set of all candidate images, and S is the Euclidean distance. For example, in Figure 1, a heuristic could be formulated as:

$$q_{12} - q_{11} = q_{22} - q_{21} \Rightarrow q_{22} = q_{21} + q_{12} - q_{11}, \quad (3)$$

which leads to $\alpha_{q_{11}} = -1$, $\alpha_{q_{12}} = 1$ and $\alpha_{q_{21}} = 1$. See Appendix C for details on selecting R and calculating α_q .

Control Baselines. We also report the random and majority-based performance for all the datasets as control baselines. These baselines allow us to put the posted performances in perspective better.

3.3 Implementation Details

We use greedy decoding (*i.e.*, no sampling) with temperature = 0.0 and top_p = 1.0 for all the tested models. Moreover, max_generation_length is set to 512 across all experiments. Furthermore, for gpt-4v, we set the model’s resolution to auto. All our experiments are carried out on a server with 4 × Quadro RTX 8000 GPUs with 48GB VRAM, 251GB RAM, and 32 CPU cores. Finally, we implemented our code using Hugging Face Transformers (Wolf et al., 2020) and PyTorch (Paszke et al., 2019) libraries.

4 How good are MLLMs at nonverbal abstract reasoning?

4.1 Exact Match Scoring

Our early observations of the responses indicated the possibility of option markers (*i.e.*, 1, 2, etc.) appearing at different token positions. For example, if the model generates “Number 4.”, the marker will be at position 3; however, if the model generates “The answer is 4.”, the marker will be at position 7. As such, we pivoted away from the common next-token scoring approach and used exact matching in our experiments. Specifically, we first extract all the numbers in the generated response and then take the earliest one as the chosen option to be compared to the ground truth. We further discuss this approach in Appendix A, providing a comparison to another common automatic scoring method.

Model	IQ50	RAVEN-S	CCSE
Pre-Trained			
blip2-opt-2.7b	0.160	0.122	0.194
blip2-opt-6.7b	0.140	0.117	0.229
blip2-flan-t5-xl	0.160	0.117	0.229
blip2-flan-t5-xxl	0.180 [‡]	0.131[‡]	0.211
idefics-9b	0.120	0.120	0.194
idefics-80b*	0.240[‡]	T	0.240
fuyu-8b	0.160	<u>0.127[‡]</u>	<u>0.297[‡]</u>
Qwen-VL	0.180 [‡]	0.117	0.206
Instruction-Tuned			
MMICL-vicuna-7b	0.200 [‡]	0.115	0.257 [‡]
MMICL-vicuna-13b*	0.180 [‡]	0.126 [‡]	0.223
MMICL-Instructblip-T5-xl	0.160	0.126 [‡]	0.229
MMICL-Instructblip-T5-xxl	0.200 [‡]	0.126 [‡]	0.229
instructblip-vicuna-7b	0.140	0.126 [‡]	0.240
instructblip-vicuna-13b*	0.160	0.117	0.217
instructblip-flan-t5-xl	0.120	0.121	0.240
instructblip-flan-t5-xxl	0.240[‡]	0.126 [‡]	0.211
idefics-9b-instruct	0.120	0.121	0.217
idefics-80b-instruct*	0.140	T	0.251 [‡]
llava-1.5-7b-hf	0.160	0.123	0.269 [‡]
llava-1.5-13b-hf*	0.240[‡]	0.121	0.229
bakLlava-v1-hf	0.080	0.122	0.314[‡]
Qwen-VL-Chat	<u>0.220[‡]</u>	0.117	0.286 [‡]
Heuristics			
Pixel	0.200	0.051	0.257
CLIP-ViT	0.480	0.099	0.234
Control Baselines			
Random	0.167	0.125	0.250
Majority	0.220	0.130	0.314

Table 1: Zero-shot accuracy on IQ50, RAVEN-S, and CCSE datasets using the generalized next-token scoring method. For each dataset, the best performance by MLLMs is **boldfaced** while the second best performance is underlined. **Legends:** T \rightarrow Timeout after one week of running, * \rightarrow Ran with half-precision (e.g., bfloat16) to fit in GPU memory, [‡] \rightarrow Performance better than the random baseline.

Table 1 presents our experimental results on IQ50, RAVEN-S, and CCSE datasets using our exact match scoring method. Our main observation from this table is that **no model consistently beats the random baselines over the three datasets**. Moreover, compared to the random baselines, the models perform within the $[-8.7\%, +7.7\%]$, $[-1.0\%, +0.6\%]$, and $[-5.6\%, +6.4\%]$ ranges for IQ50, RAVEN-S, and CCSE, respectively. Although some models achieve non-trivial gains over the random baselines and even outperform some of the heuristic baselines, these results expose the difficulty of solving variations of the RPM-style questions across a wide range of MLLMs.

Looking at the results posted by the pre-trained

models, apart from fuyu-8b, we cannot observe a significant difference between the multi-task pre-trained models and the BLIP-2 family. Moreover, comparing the best-achieved performances with the majority baselines, we observe a stark similarity ($\pm 2\%$). This begs the question of whether the posted numbers are true representatives of the reasoning powers of MLLMs or simply a side-effect of their generation biases (e.g., a model that always generates 1s will do very well on a dataset with many 1s as gold labels). To this end, in [subsection 4.2](#), we will manually examine the generated answers by the instruction-tuned models.

It is also worth noting that, by examining the results posted within and beyond the same family of models, we observe that the scaling law in terms of model size (Kaplan et al., 2020) (i.e., the larger the model, the higher the performance) does not hold here. [Figure 2](#) illustrates the models’ zero-shot accuracy concerning the number of parameters.

4.2 Manual Scoring

One critical aspect of assessing such models’ abilities is ensuring the correctness and faithfulness of their reasoning. As such, we manually inspect the generated responses to provide insights into the results posted by the models in the exact match scoring schemes. All the inspections were done by a group of three graduate students (See [Appendix D](#) for the rubric). Moreover, to elicit reasoning, we appended the phrase “*Let’s think step by step.*” to the prompt (Kojima et al., 2022). Out of the 14 open-source instruction-tuned models (See [Table 3](#)), we were only able to get meaningful and coherent responses from the following models: llava-1.5-7b-hf, llava-1.5-13b-hf, Qwen-VL-Chat, and idefics-9b-instruct. Besides these models, we also manually measured the abstract reasoning abilities of closed-source MLLMs (i.e., gpt-4v and gemini-pro-vision), as we don’t have access to their generated logits corresponding to the correct answer. For the remainder of our experiments, we relied on IQ50 as it is a small challenging test set that is easy for humans to solve but difficult for MLLMs (See [Table 1](#)). This choice also allows us to more easily expand our study with a variety of experiments.

[Table 2](#) presents the performance of the aforementioned models on IQ50, demonstrating their poor explicit reasoning capabilities. More specifically, only one of the open-source instruction-tuned models achieves a non-zero performance on the

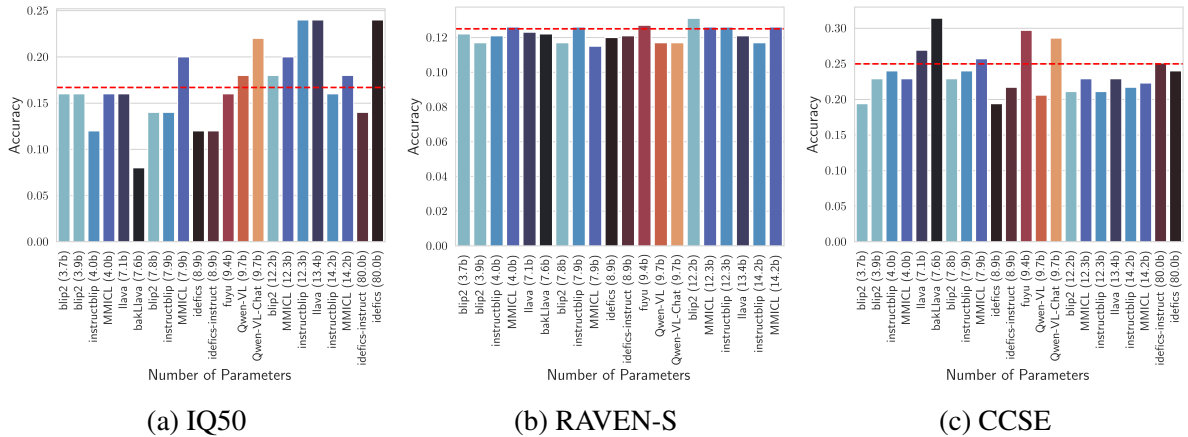


Figure 2: Zero-shot accuracy concerning the number of parameters using the exact match scoring method. Models are sorted from smallest (left) to largest (right), and those within the same family are colored the same. The red dashed lines indicate the random baselines.

Model	$\checkmark A$	$\checkmark R$	$\times A$	$\checkmark R$	$\checkmark A$	$\times R$
gpt-4v	0.26	0.16	<u>0.10</u>			
gemini-pro-vision	<u>0.10</u>		<u>0.14</u>			0.16
llava-1.5-7b-hf	0.00	0.00	0.02			
llava-1.5-13b-hf	0.04	0.02	0.10			
idefics-9b-instruct	0.00	0.00	0.08			
Qwen-VL-Chat	0.00	0.00	0.04			

Table 2: Performances of instruction-tuned models on IQ50, assessed by manual inspection, in terms of **A**nswer and **R**easoning correctness, indicated by **A** and **R**, respectively. The best performance is **boldfaced** while the second best performance is underlined.

joint answer and reasoning correctness, with an abysmal performance of 4%, (*i.e.*, an average of 1% across open-source models). Meanwhile, the trend in the closed-source MLLMs is more promising, with gpt-4v outperforming random and majority baseline, providing correct reasoning and answers in 26% of the samples. Nevertheless, their performance still lags behind the simple heuristics by a large margin (See Table 1). Regarding the faithfulness of answers to reasonings, we only observe a meaningful level of faithfulness (alignment between reasoning and answer when either is correct) in closed-source models, 50% for gpt-4v and 25% for gemini-pro-vision. Observing such a high percentage of unfaithfulness to reasoning further asserts the importance of conducting manual evaluations rather than merely reporting performances using noisy automatic measurements.

During our inspections, we observed that although models generally understand the shapes in the query images, they tend to hallucinate about

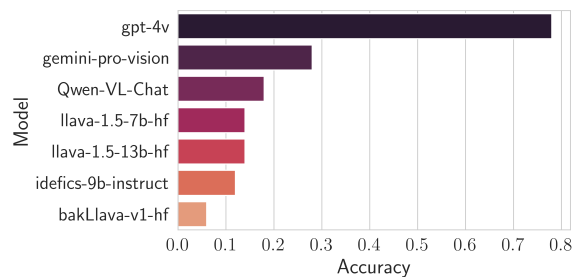


Figure 3: Zero-shot CoT accuracy on IQ50 using text-only prompts.

specific features such as rotation, shadows, and orientations. On the reasoning side, the most prominent issue was the models being overly descriptive rather than being focused on providing grounded logical reasoning. In other words, most of the time, the generated responses were the descriptions of the puzzle and the candidate options. We believe this to be an artifact of their training datasets; however, we expected a much better showing from the models that receive multi-task training (See Table 3).

5 What is holding MLLMs back?

5.1 Textual Reasoning

Since most MLLMs fuse the information from visual and textual modalities, they are prone to error propagation from each. Hence, if we bypass one module, we can effectively evaluate the remaining one. For the textual module, we can do this by providing the text-only version of each sample (*i.e.*, the textual description of the puzzles) written by a human expert (See Appendix F for examples). Through these experiments, we can gain

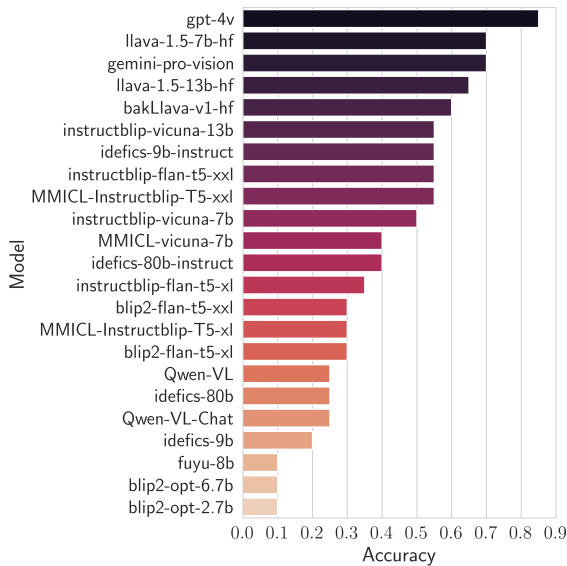


Figure 4: Visual awareness questions performances on a subset of IQ50.

insights into the ceiling reasoning capabilities of each model. In our experiments, due to their incompatibility with text-only prompts, we had to drop MMICL* and InstructBLIP* models. Moreover, we dropped `idefics-80b-instruct` as we could not elicit reasonings from it.

Figure 3 presents a comparison between open-source and closed-source MLLMs on IQ50 using text-only zero-shot CoT prompts. As evident, `gpt-4v` is the only model that achieves a high level of performance, with `gemi-pro-vision` coming in as a distant second. These results are consistent with our previous observations, where open-source models struggled to achieve good results, showcasing a lack of textual reasoning abilities.

5.2 Visual Awareness

Correctly perceiving visual details is critical to non-verbal abstract reasoning. However, Zhang et al. (2023a) have shown that MLLMs face difficulties when isolating granular details in large images. As such, we ran a set of experiments to determine the extent to which our tested MLLMs understand the presented puzzles. More concretely, we developed 20 questions designed to test the models on understanding shape, relative position, orientation, color, filling pattern, and fine-grained details. In our experiments, we dropped `MMICL-vicuna-13b` as we could not elicit proper responses.

Figure 4 presents the performances posted on the visual awareness questions across open-source and closed-source models. As evident, `gpt-4v`

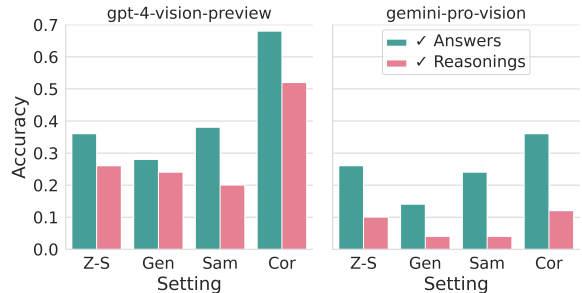


Figure 5: Guided prompting performance of `gpt-4v` and `gemi-pro-vision` on IQ50 using different types of hints. **Legend:** Z-S → Zero-shot, Gen → General, Sam → Sample-specific, and Cor → Corrective.

dominates the benchmark with a comfortable lead; however, we find it very promising that some open-source models such as `llava*` can keep up with the other closed-source model (*i.e.*, `gemi-pro-vision`). Overall, observing the low performances of open-source MLLMs in visual awareness and textual reasoning paints a clearer picture of models’ shortcomings, explaining their results in Section 4.

6 Can MLLMs’ reasoning be improved?

6.1 Guided Prompting

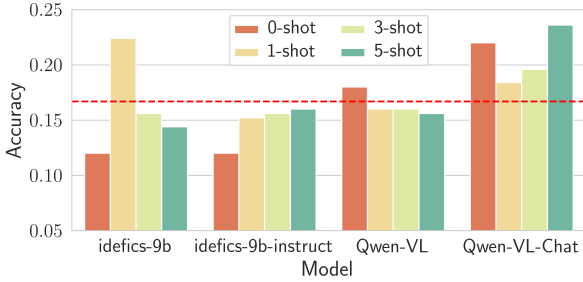
Prompt engineering has been one of the prominent methods to guide LLMs towards specific desired outputs through better conditioning (Wei et al., 2022; Kojima et al., 2022; Wang et al., 2023b; Li et al., 2023b). We experiment with three guided prompting setups, each providing the models with different cues to understand how supplementary textual information is utilized while generating responses. The three setups are as follows (See Appendix F for examples):

General. In this setup, we provide the models with broad cues on approaching such visual puzzles, hinting at the common strategies without being sample-specific.

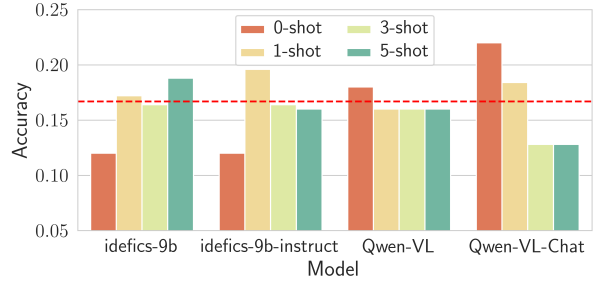
Sample-specific. In this setup, we provide the models with one sample-specific hint about the desired reasoning for solving each puzzle.

Corrective. In this setup, in an interactive process, looking at the model’s reasoning when prompted in a zero-shot setting, we add one hint to correct the most prominent error.

Figure 5 illustrates the performance of closed-source models on IQ50 given different hints. Looking at these results, we find sample-specific and



(a) In-Distribution



(b) Out-of-Distribution

Figure 6: Zero-shot and symmetrical few-shot accuracy on IQ50. In (a) *In-Distribution*, the demonstrations are taken from IQ50, while in (b) *Out-of-Distribution*, the demonstrations are taken from RAVEN-S. Each variation was executed five times with different seeds to mitigate the effect of random sampling. The red dashed lines indicate the random baselines.

general hints detrimental to reasoning and accuracy while observing a significant boost when interactively utilizing corrective hints, especially for gpt-4v. Considering the distinct embedded cues of sample-specific and corrective hints, we believe that the models’ inherent chain of reasoning on the provided puzzles is misaligned with humans, which makes sample-specific hints confusing rather than helpful. However, we can correct models’ already laid out solutions with corrective hints, improving their performance by as much as 100%.

6.2 In-Context Learning

In-context learning (ICL) refers to emergent behavior in LLMs where they perform a task conditioned on the provided demonstrations without further parameter optimization. Min et al. (2022) have suggested that ICL is a mere mechanism for locating the already learned ability of the model to respond to the query prompt. However, more recent studies (Garg et al., 2022; Mirchandani et al., 2023; Lee et al., 2023) have shown that LLMs can learn various function classes through ICL.

6.2.1 Symmetrical Few-Shot Learning

The most common form of ICL is few-shot learning, in which the model is provided with demonstrations similar to the test sample. We call this variation “Symmetrical” as there is no imbalance in the demonstrations’ textual and visual information pieces. Since symmetrical ICL requires processing multiple image and text pairs, we only utilize models capable of processing such inputs (See Table 3 for a list). Moreover, due to burdensome computation costs, we exclude idefics-80b* models. In our experiments, we explored the effect of 1) changing the sampling distribution of demonstra-

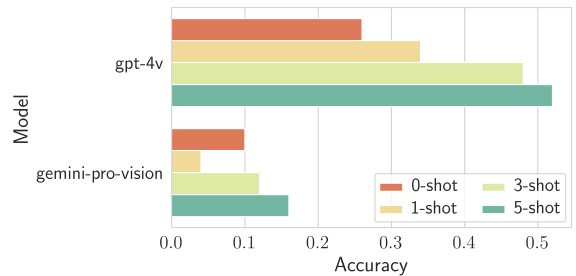


Figure 7: Symmetrical few-shot CoT accuracy on IQ50.

tions and 2) including step-by-step reasoning with demonstrations (See Appendix F for examples).

Effect of sampling distribution. Our experiments cover open-source models and utilize the exact match scoring scheme over two variations: 1) *In-Distribution (ID)*: demonstrations are uniformly taken from the same dataset, and 2) *Out-of-Distribution (OOD)*: demonstrations are uniformly taken from another dataset. We used IQ50 as the primary evaluation source alongside RAVEN-S as the OOD source. Moreover, we ran each variation five times to lessen the impact of random sampling and with up to five demonstrations (*i.e.*, 10% of the dataset) due to GPU limits.

Figure 6 presents the results of our experiments. As evident, there are no consistent patterns across models and variations. For example, while idefics-9b* models generally benefit from the few-shot scheme, we don’t see monotonically increasing performances with more demonstrations, contrary to expected patterns in LLMs. Simultaneously, we see a consistent decline in performance in some variations of Qwen-VL* models. We believe these irregularities are caused by an inability

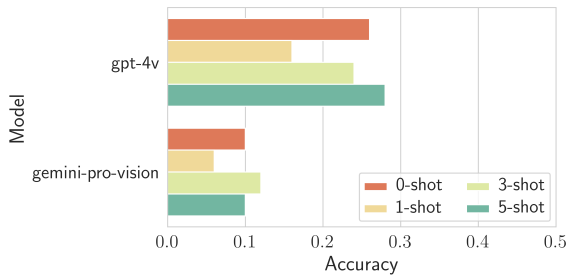


Figure 8: Asymmetrical few-shot CoT accuracy on IQ50.

to understand the utility of the demonstrations, suggesting that the tested models do not exhibit strong and consistent symmetrical ICL capabilities. As a result, the models cannot take advantage of the provided demonstrations properly, leading to poor responses and subpar performances.

Effect of step-by-step reasoning. Inspired by its success, we experiment with the few-shot Chain-of-Thought (CoT) prompting (Wei et al., 2022) to improve the performance of our models. Our early experiments found open-source models, such as Qwen-VL-Chat and idfics-9b-instruct, unable to comprehend CoT prompting. As such, we focused on examining the closed-source models: gpt-4v and gemini-pro-vision.

Figure 7 presents the performance of closed-source models with CoT prompting. We can observe that both models benefit significantly from CoT demonstrations, with gpt-4v’s performance being boosted as much as 100%. These results emphasize the immense gap between the open-source and closed-source models while showcasing meaningful symmetrical ICL abilities in these models. During our inspections, we noticed an unusual phenomenon with gemini-pro-vision in which the one-shot variation prevented the model from generating reasonings in almost all the examples, leading to an initial performance drop. Moreover, in a similar setting for gpt-4v, we observed 1) a massive jump in the number of safeguard triggers (4% → 18%), which precluded the model from generating a response, and 2) an increased confusion regarding the boundaries of the provided demonstration (0% → 10%), diminishing the model’s performance.

6.2.2 Asymmetrical Few-Shot Learning

Adding new modalities has brought forth the possibility of providing lopsided (*i.e.*, Asymmetrical) information in the input prompt. As such, we con-

duct a set of few-shot experiments that provide the models with text-only CoT demonstrations while keeping the query unchanged (*i.e.*, image + text). To encourage the models to use the demonstrations, we append “Let’s solve the puzzle in the image, step by step, similar to the demonstrations.” to our prompt. We hypothesize that similar to the findings of Min et al. (2022), the models will better understand the input and output spaces and achieve improved performance.

Since we could not make open-source models properly utilize the textual demonstrations in our preliminary experiments, we continued our experiments only on closed-source models. Figure 8 illustrates the results of our experiments with asymmetrical few-shot CoT prompting. As evident, this approach does not yield meaningful improvements and even causes degradation in some cases, contrasting our hypothesis. Moreover, we noticed increased hallucinations, mostly confusing the demonstrations with queries and detecting non-existent details in the shapes, leading to unfaithfulness and instability in the responses. We leave further investigations to future works.

7 Conclusion

In this study, we utilized different RPM-style tasks as a proxy for measuring the nonverbal abstract reasoning abilities of MLLMs, covering 24 different open-source and closed-source models. Although closed-source MLLMs showcased promising capabilities in our experiments, we found the abilities of open-source models to be insufficient for solving these tasks. Moreover, using pseudo-isolated experimental environments, we found that MLLMs often fail at 1) gathering precise visual details from puzzles and 2) reasoning correctly and faithfully, even when provided with expert-written and complete descriptions of the puzzles. Furthermore, our experiments highlighted the inability of open-source models to consistently utilize demonstrations and the ICL prowess of the closed-source models, which helped them benefit from interactive guidance or provided demonstrations with step-by-step (*i.e.*, CoT) reasoning. Although MLLMs have previously demonstrated proficiency at various tasks, our study using a relatively simple reasoning task for humans has exposed some critical shortcomings in MLLMs while highlighting the importance of more grounded evaluations, even at small scales.

Limitations

In this work, we focused on only a specific type of reasoning task (*i.e.*, nonverbal abstract reasoning) while using only IQ50, a small but challenging dataset, in most of our experiments. However, despite these limitations, we hypothesize that similar shortcomings could be replicated in other reasoning tasks due to the fundamental and not task-specific nature of the observed problems. Moreover, although our experiments yielded insightful results, further analysis of the observations is still possible. For example, given the remarkable effectiveness of corrective hints, we can utilize methods such as self-talk (Press et al., 2023), automating the whole process. Another example is the visual awareness tests, where it is possible to examine the internal values of the models (*e.g.*, attention weights, token probabilities, etc.), as opposed to evaluating the generated responses. Finally, since the closed-source models’ training datasets are unknown, test set contamination is possible, leading to their superior performance. However, based on the relatively low performance of these models and considering the low-level difficulty of the tests for humans, we believe contamination to be unlikely.

Ethics Statement

This work does not have any ethical considerations.

Acknowledgements

This work has been sponsored and funded by the Defense Advanced Research Projects Agency via contract HR00112390061 and award N660011924033.

References

- Jean-Baptiste Alayrac, Jeff Donahue, Pauline Luc, Antoine Miech, Iain Barr, Yana Hasson, Karel Lenc, Arthur Mensch, Katherine Millican, Malcolm Reynolds, et al. 2022. Flamingo: a visual language model for few-shot learning. *Advances in Neural Information Processing Systems*, 35:23716–23736.
- Jinze Bai, Shuai Bai, Shusheng Yang, Shijie Wang, Sinan Tan, Peng Wang, Junyang Lin, Chang Zhou, and Jingren Zhou. 2023. Qwen-vl: A frontier large vision-language model with versatile abilities. *arXiv preprint arXiv:2308.12966*.
- David Barrett, Felix Hill, Adam Santoro, Ari Morcos, and Timothy Lillicrap. 2018. Measuring abstract reasoning in neural networks. In *International conference on machine learning*, pages 511–520. PMLR.
- Rohan Bavishi, Erich Elsen, Curtis Hawthorne, Maxwell Nye, Augustus Odena, Arushi Somani, and Saġnak Taşirlar. 2023. [Introducing our multimodal models](#).
- Laura E Berk. 1994. Why children talk to themselves. *Scientific American*, 271(5):78–83.
- Tom Brown, Benjamin Mann, Nick Ryder, Melanie Subbiah, Jared D Kaplan, Prafulla Dhariwal, Arvind Neelakantan, Pranav Shyam, Girish Sastry, Amanda Askell, et al. 2020. Language models are few-shot learners. *Advances in neural information processing systems*, 33:1877–1901.
- Sébastien Bubeck, Varun Chandrasekaran, Ronen Eldan, Johannes Gehrike, Eric Horvitz, Ece Kamar, Peter Lee, Yin Tat Lee, Yuanzhi Li, Scott Lundberg, et al. 2023. Sparks of artificial general intelligence: Early experiments with gpt-4. *arXiv preprint arXiv:2303.12712*.
- Raymond Bernard Cattell. 1987. *Intelligence: Its structure, growth and action*. Elsevier.
- Xi Chen, Xiao Wang, Soravit Changpinyo, AJ Piergiovanni, Piotr Padlewski, Daniel Salz, Sebastian Goodman, Adam Grycner, Basil Mustafa, Lucas Beyer, et al. 2022. Pali: A jointly-scaled multilingual language-image model. *arXiv preprint arXiv:2209.06794*.
- Cédric Colas, Tristan Karch, Clément Moulin-Frier, and Pierre-Yves Oudeyer. 2021. [Language as a cognitive tool: Dall-e, humans and vygotskian rl agents](#).
- Wenliang Dai, Junnan Li, Dongxu Li, Anthony Meng Huat Tiong, Junqi Zhao, Weisheng Wang, Boyang Li, Pascale Fung, and Steven Hoi. 2023. [Instructblip: Towards general-purpose vision-language models with instruction tuning](#).
- Alexey Dosovitskiy, Lucas Beyer, Alexander Kolesnikov, Dirk Weissenborn, Xiaohua Zhai, Thomas Unterthiner, Mostafa Dehghani, Matthias Minderer, Georg Heigold, Sylvain Gelly, Jakob Uszkoreit, and Neil Houlsby. 2021. [An image is worth 16x16 words: Transformers for image recognition at scale](#). In *International Conference on Learning Representations*.
- Alexey Dosovitskiy, Lucas Beyer, Alexander Kolesnikov, Dirk Weissenborn, Xiaohua Zhai, Thomas Unterthiner, Mostafa Dehghani, Matthias Minderer, Georg Heigold, Sylvain Gelly, et al. 2020. An image is worth 16x16 words: Transformers for image recognition at scale. *arXiv preprint arXiv:2010.11929*.
- Shivam Garg, Dimitris Tsipras, Percy S Liang, and Gregory Valiant. 2022. What can transformers learn in-context? a case study of simple function classes. *Advances in Neural Information Processing Systems*, 35:30583–30598.
- Gemini Team Google. 2023. [Gemini: A family of highly capable multimodal models](#).

- Xiaotian Han, Quanzeng You, Yongfei Liu, Wentao Chen, Huangjie Zheng, Khalil Mrini, Xudong Lin, Yiqi Wang, Bohan Zhai, Jianbo Yuan, et al. 2023. Core-mm: Complex open-ended reasoning evaluation for multi-modal large language models. *arXiv preprint arXiv:2311.11567*.
- Yaru Hao, Haoyu Song, Li Dong, Shaohan Huang, Zewen Chi, Wenhui Wang, Shuming Ma, and Furu Wei. 2022. Language models are general-purpose interfaces. *arXiv preprint arXiv:2206.06336*.
- Valentin Hartmann, Anshuman Suri, Vincent Bindschaedler, David Evans, Shruti Tople, and Robert West. 2023. Sok: Memorization in general-purpose large language models. *arXiv preprint arXiv:2310.18362*.
- Felix Hill, Adam Santoro, David GT Barrett, Ari S Morcos, and Timothy Lillicrap. 2019. Learning to make analogies by contrasting abstract relational structure. *arXiv preprint arXiv:1902.00120*.
- Xiaoyang Hu, Shane Storks, Richard L Lewis, and Joyce Chai. 2023. In-context analogical reasoning with pre-trained language models. *arXiv preprint arXiv:2305.17626*.
- Shaohan Huang, Li Dong, Wenhui Wang, Yaru Hao, Saksham Singhal, Shuming Ma, Tengchao Lv, Lei Cui, Owais Khan Mohammed, Qiang Liu, et al. 2023. Language is not all you need: Aligning perception with language models. *arXiv preprint arXiv:2302.14045*.
- Marius Jahrens and Thomas Martinetz. 2020. Solving raven’s progressive matrices with multi-layer relation networks. In *2020 International Joint Conference on Neural Networks (IJCNN)*, pages 1–6. IEEE.
- Jared Kaplan, Sam McCandlish, Tom Henighan, Tom B. Brown, Benjamin Chess, Rewon Child, Scott Gray, Alec Radford, Jeffrey Wu, and Dario Amodei. 2020. [Scaling laws for neural language models](#).
- Mehran Kazemi, Hamidreza Alvari, Ankit Anand, Jialin Wu, Xi Chen, and Radu Soricut. 2023. Geomverse: A systematic evaluation of large models for geometric reasoning. *arXiv preprint arXiv:2312.12241*.
- Takeshi Kojima, Shixiang Shane Gu, Machel Reid, Yutaka Matsuo, and Yusuke Iwasawa. 2022. Large language models are zero-shot reasoners. *Advances in neural information processing systems*, 35:22199–22213.
- Hugo Laurençon, Lucile Saulnier, Léo Tronchon, Stas Bekman, Amanpreet Singh, Anton Lozhkov, Thomas Wang, Siddharth Karamcheti, Alexander M. Rush, Douwe Kiela, Matthieu Cord, and Victor Sanh. 2023. [Obelics: An open web-scale filtered dataset of interleaved image-text documents](#).
- Dong-Ho Lee, Kian Ahrabian, Woojeong Jin, Fred Morstatter, and Jay Pujara. 2023. [Temporal knowledge graph forecasting without knowledge using in-context learning](#). In *Proceedings of the 2023 Conference on Empirical Methods in Natural Language Processing*, pages 544–557, Singapore. Association for Computational Linguistics.
- Junnan Li, Dongxu Li, Silvio Savarese, and Steven Hoi. 2023a. Blip-2: Bootstrapping language-image pre-training with frozen image encoders and large language models. *arXiv preprint arXiv:2301.12597*.
- Junnan Li, Dongxu Li, Caiming Xiong, and Steven Hoi. 2022. Blip: Bootstrapping language-image pre-training for unified vision-language understanding and generation. In *International Conference on Machine Learning*, pages 12888–12900. PMLR.
- Zekun Li, Baolin Peng, Pengcheng He, Michel Galley, Jianfeng Gao, and Xifeng Yan. 2023b. [Guiding large language models via directional stimulus prompting](#). In *Thirty-seventh Conference on Neural Information Processing Systems*.
- Haotian Liu, Chunyuan Li, Qingyang Wu, and Yong Jae Lee. 2023a. Visual instruction tuning. *arXiv preprint arXiv:2304.08485*.
- Yuliang Liu, Zhang Li, Hongliang Li, Wenwen Yu, Mingxin Huang, Dezhi Peng, Mingyu Liu, Mingrui Chen, Chunyuan Li, Lianwen Jin, et al. 2023b. On the hidden mystery of ocr in large multimodal models. *arXiv preprint arXiv:2305.07895*.
- Hongjing Lu, Nicholas Ichien, and Keith J Holyoak. 2022. Probabilistic analogical mapping with semantic relation networks. *Psychological review*.
- Pan Lu, Hritik Bansal, Tony Xia, Jiacheng Liu, Chunyuan Li, Hannaneh Hajishirzi, Hao Cheng, Kai-Wei Chang, Michel Galley, and Jianfeng Gao. 2024. [Mathvista: Evaluating mathematical reasoning of foundation models in visual contexts](#). In *The Twelfth International Conference on Learning Representations*.
- Gary Lupyan. 2012. What do words do? toward a theory of language-augmented thought. In *Psychology of learning and motivation*, volume 57, pages 255–297. Elsevier.
- Sewon Min, Xinxu Lyu, Ari Holtzman, Mikel Artetxe, Mike Lewis, Hannaneh Hajishirzi, and Luke Zettlemoyer. 2022. [Rethinking the role of demonstrations: What makes in-context learning work?](#) In *Proceedings of the 2022 Conference on Empirical Methods in Natural Language Processing*, pages 11048–11064, Abu Dhabi, United Arab Emirates. Association for Computational Linguistics.
- Suvir Mirchandani, Fei Xia, Pete Florence, Brian Ichter, Danny Driess, Montserrat Gonzalez Arenas, Kanishka Rao, Dorsa Sadigh, and Andy Zeng. 2023. Large language models as general pattern machines. *arXiv preprint arXiv:2307.04721*.

- Melanie Mitchell, Alessandro B Palmarini, and Arseny Moskvichev. 2023. Comparing humans, gpt-4, and gpt-4v on abstraction and reasoning tasks. *arXiv preprint arXiv:2311.09247*.
- Hyeonseob Nam, Jung-Woo Ha, and Jeonghee Kim. 2017. Dual attention networks for multimodal reasoning and matching. In *Proceedings of the IEEE conference on computer vision and pattern recognition*, pages 299–307.
- OpenAI. 2023. [Gpt-4 technical report](#).
- Adam Paszke, Sam Gross, Francisco Massa, Adam Lerer, James Bradbury, Gregory Chanan, Trevor Killeen, Zeming Lin, Natalia Gimelshein, Luca Antiga, et al. 2019. Pytorch: An imperative style, high-performance deep learning library. *Advances in neural information processing systems*, 32.
- Ofir Press, Muru Zhang, Sewon Min, Ludwig Schmidt, Noah Smith, and Mike Lewis. 2023. [Measuring and narrowing the compositionality gap in language models](#). In *Findings of the Association for Computational Linguistics: EMNLP 2023*, pages 5687–5711, Singapore. Association for Computational Linguistics.
- Zhangyang Qi, Ye Fang, Mengchen Zhang, Zeyi Sun, Tong Wu, Ziwei Liu, Dahua Lin, Jiaqi Wang, and Hengshuang Zhao. 2023. Gemini vs gpt-4v: A preliminary comparison and combination of vision-language models through qualitative cases. *arXiv preprint arXiv:2312.15011*.
- Alec Radford, Jong Wook Kim, Chris Hallacy, Aditya Ramesh, Gabriel Goh, Sandhini Agarwal, Girish Sastry, Amanda Askell, Pamela Mishkin, Jack Clark, et al. 2021. Learning transferable visual models from natural language supervision. In *International conference on machine learning*, pages 8748–8763. PMLR.
- Alec Radford, Jeffrey Wu, Rewon Child, David Luan, Dario Amodei, Ilya Sutskever, et al. 2019. Language models are unsupervised multitask learners. *OpenAI blog*, 1(8):9.
- Jean Raven. 2003. Raven progressive matrices. In *Handbook of nonverbal assessment*, pages 223–237. Springer.
- Christopher Rytting and David Wingate. 2021. Leveraging the inductive bias of large language models for abstract textual reasoning. *Advances in Neural Information Processing Systems*, 34:17111–17122.
- Mohammed K Shakeel, Vina M Goghari, et al. 2017. Measuring fluid intelligence in healthy older adults. *Journal of Aging Research*, 2017.
- Ashish Vaswani, Noam Shazeer, Niki Parmar, Jakob Uszkoreit, Llion Jones, Aidan N Gomez, Łukasz Kaiser, and Illia Polosukhin. 2017. Attention is all you need. *Advances in neural information processing systems*, 30.
- Lev Vygotsky. 1962. *Thought and language*. MIT Press Cambridge, MA.
- Andrey Vyshedskiy. 2019. Language evolution to revolution: the leap from rich-vocabulary non-recursive communication system to recursive language 70,000 years ago was associated with acquisition of a novel component of imagination, called prefrontal synthesis, enabled by a mutation that slowed down the prefrontal cortex maturation simultaneously in two or more children—the romulus and remus hypothesis. *Research Ideas and Outcomes*, 5:e38546.
- Jiaqi Wang, Zhengliang Liu, Lin Zhao, Zihao Wu, Chong Ma, Sigang Yu, Haixing Dai, Qiushi Yang, Yiheng Liu, Songyao Zhang, et al. 2023a. Review of large vision models and visual prompt engineering. *Meta-Radiology*, page 100047.
- Lei Wang, Wanyu Xu, Yihuai Lan, Zhiqiang Hu, Yunshi Lan, Roy Ka-Wei Lee, and Ee-Peng Lim. 2023b. [Plan-and-solve prompting: Improving zero-shot chain-of-thought reasoning by large language models](#). In *Proceedings of the 61st Annual Meeting of the Association for Computational Linguistics (Volume 1: Long Papers)*, pages 2609–2634, Toronto, Canada. Association for Computational Linguistics.
- Wenhui Wang, Hangbo Bao, Li Dong, Johan Bjorck, Zhiliang Peng, Qiang Liu, Kriti Aggarwal, Owais Khan Mohammed, Saksham Singhal, Subhojit Som, et al. 2022. Image as a foreign language: Beit pretraining for all vision and vision-language tasks. *arXiv preprint arXiv:2208.10442*.
- Taylor Webb, Keith J Holyoak, and Hongjing Lu. 2023. Emergent analogical reasoning in large language models. *Nature Human Behaviour*, 7(9):1526–1541.
- Jason Wei, Xuezhi Wang, Dale Schuurmans, Maarten Bosma, brian ichter, Fei Xia, Ed H. Chi, Quoc V Le, and Denny Zhou. 2022. [Chain of thought prompting elicits reasoning in large language models](#). In *Advances in Neural Information Processing Systems*.
- Jonathan Winawer, Nathan Witthoft, Michael C Frank, Lisa Wu, Alex R Wade, and Lera Boroditsky. 2007. Russian blues reveal effects of language on color discrimination. *Proceedings of the national academy of sciences*, 104(19):7780–7785.
- Thomas Wolf, Lysandre Debut, Victor Sanh, Julien Chaumond, Clement Delangue, Anthony Moi, Pierric Cistac, Tim Rault, Remi Louf, Morgan Funtowicz, Joe Davison, Sam Shleifer, Patrick von Platen, Clara Ma, Yacine Jernite, Julien Plu, Canwen Xu, Teven Le Scao, Sylvain Gugger, Mariama Drame, Quentin Lhoest, and Alexander Rush. 2020. [Transformers: State-of-the-art natural language processing](#). In *Proceedings of the 2020 Conference on Empirical Methods in Natural Language Processing: System Demonstrations*, pages 38–45, Online. Association for Computational Linguistics.
- Xiang Yue, Yuansheng Ni, Kai Zhang, Tianyu Zheng, Ruoqi Liu, Ge Zhang, Samuel Stevens, Dongfu Jiang, Weiming Ren, Yuxuan Sun, et al. 2023. Mmmu:

A massive multi-discipline multimodal understanding and reasoning benchmark for expert agi. *arXiv preprint arXiv:2311.16502*.

Chi Zhang, Feng Gao, Baoxiong Jia, Yixin Zhu, and Song-Chun Zhu. 2019. Raven: A dataset for relational and analogical visual reasoning. In *Proceedings of the IEEE/CVF conference on computer vision and pattern recognition*, pages 5317–5327.

Jiarui Zhang, Mahyar Khayatkhoei, Prateek Chhikara, and Filip Ilievski. 2023a. Visual cropping improves zero-shot question answering of multimodal large language models. *arXiv preprint arXiv:2310.16033*.

Yuanhan Zhang, Kaiyang Zhou, and Ziwei Liu. 2023b. What makes good examples for visual in-context learning? *arXiv preprint arXiv:2301.13670*.

Haozhe Zhao, Zefan Cai, Shuzheng Si, Xiaojian Ma, Kaikai An, Liang Chen, Zixuan Liu, Sheng Wang, Wenjuan Han, and Baobao Chang. 2023. Mmicl: Empowering vision-language model with multi-modal in-context learning. *arXiv preprint arXiv:2309.07915*.

Deyao Zhu, Jun Chen, Xiaoqian Shen, Xiang Li, and Mohamed Elhoseiny. 2023a. [Minigt-4: Enhancing vision-language understanding with advanced large language models](#).

Yutao Zhu, Huaying Yuan, Shuting Wang, Jiongnan Liu, Wenhan Liu, Chenlong Deng, Zhicheng Dou, and Ji-Rong Wen. 2023b. Large language models for information retrieval: A survey. *arXiv preprint arXiv:2308.07107*.

Tao Zhuo and Mohan Kankanhalli. 2020. Solving raven’s progressive matrices with neural networks. *arXiv preprint arXiv:2002.01646*.

A One-by-One Scoring

Introduced by [Huang et al. \(2023\)](#), in this scoring method, we first flatten the query image matrix and feed it into the model along with exactly one option. We also surround these images with textual instructions to help the model better understand the desired task (See [Appendix F](#) for examples). Then, we calculate the probability of the model generating “Yes”, representing the probability of that option being the true missing piece. Finally, we determine the model’s choice by taking the option with the highest probability. To improve the original method, we introduce an equivalency condition in which the max probability of different variations of the target token (*e.g.*, “YES” and “yes”) is taken as the probability. The main shortcomings of this method include 1) being more computation-heavy as it needs to process each option separately and 2) being compatible with only the models that accept

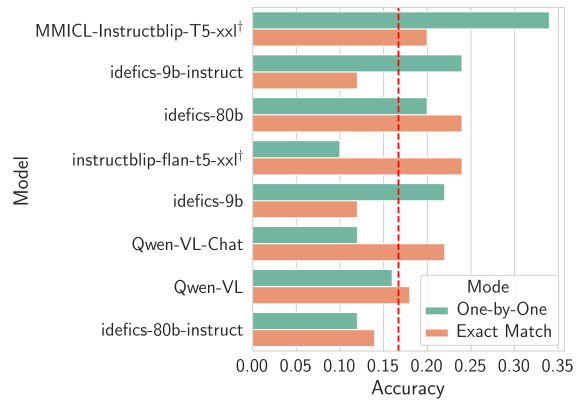


Figure 9: Zero-shot accuracy comparison on the IQ50 dataset using the one-by-one and the generalized next-token scoring methods. Results with a † marker are taken from [Zhao et al. \(2023\)](#). Due to runtime errors, we could not replicate them (neither Huggingface nor GitHub versions). The red dashed line indicates the random baseline.

multiple images as input. Notably, among the open-source models utilized in this study, only Qwen-VL* and idefics* models support multi-image inputs (See [Table 3](#)).

[Figure 9](#) compares the experimental results with this and generalized next-token scoring methods. As evident, some models such as MMICL-Instructblip-T5-xxl, idefics-9b, and idefics-9b-instruct benefit significantly from this scoring mode, while others such as instructblip-flan-t5-xxl and Qwen-VL-Chat suffer extensively. This observation demonstrates the validity of both methods, making the choice subject to the task/dataset being evaluated. However, given these mixed results and the downsides of using this scoring method, we conclude that the generalized next-token scoring method is more practical for future studies.

B Models

[Table 3](#) presents an attribute comparison over open-source and closed-source models.

BLIP-2 (Li et al., 2023a). BLIP-2 is a generic and efficient pre-training strategy that bootstraps vision-language pre-training from off-the-shelf frozen pre-trained image encoders and frozen large language models. BLIP-2 bridges the modality gap with a lightweight Querying Transformer, which is pre-trained in two stages. Despite having significantly fewer trainable parameters than existing methods, BLIP-2 achieves state-of-the-art perfor-

mance on various vision-language tasks.

Fuyu (Bavishi et al., 2023). Fuyu is a multi-modal text and image transformer trained by Adept AI. Architecturally, Fuyu is a vanilla decoder-only transformer with no image encoder. Image patches are instead linearly projected into the first layer of the transformer, bypassing the embedding lookup. This simplification allows the model to support arbitrary image resolutions. Fuyu-8B improves over Qwen-VL on 2 out of the 3 most commonly used image-understanding datasets despite having 2B fewer parameters.

IDEFICS (Laurençon et al., 2023). IDEFICS (Image-aware Decoder Enhanced à la Flamingo with Interleaved Cross-attentionS) is an open-access reproduction of Flamingo, a closed-source visual language model developed by Deepmind. It is built on top of two unimodal open-access pre-trained models with newly initialized parameters in the form of Transformer blocks to bridge the gap between the vision encoder and the language model. The model is trained on image-text pairs and unstructured multi-modal web documents. IDEFICS-instruct is the model obtained by further training IDEFICS on Supervised Fine-Tuning and Instruction Fine-Tuning datasets. IDEFICS is on par with the original closed-source model on various image-text benchmarks, including visual question answering (open-ended and multiple choice), image captioning, and image classification when evaluated with in-context few-shot learning.

Qwen-VL (Bai et al., 2023). Qwen-VL models are large-scale vision-language models (LVLMs) designed to perceive and understand texts and images. Starting from the Qwen-LM as a foundation, the model is endowed with visual capacity by the meticulously designed (i) visual receptor, (ii) input-output interface, (iii) 3-stage training pipeline, and (iv) multilingual multi-modal cleaned corpus. The resulting models, including Qwen-VL and Qwen-VL-Chat, set new records for generalist models under similar model scales.

InstructBLIP (Dai et al., 2023). InstructBLIP models are instruction-tuned MLLMs based on the pre-trained BLIP-2 models. They have been trained using 26 publicly available datasets transformed into instruction tuning format. Additionally, the authors introduce an instruction-aware Query Transformer, which extracts informative features tailored to the given instruction. Trained on 13

Model	Size	Open Source	Multi-Task Pre-Training	Multi-Image Input
Pre-Trained				
blip2-opt-2.7b	3.7b	✓	✗	✗
blip2-opt-6.7b	7.8b	✓	✗	✗
blip2-flan-t5-x1	3.9b	✓	✗	✗
blip2-flan-t5-xxl	12.2b	✓	✗	✗
idefics-9b	8.9b	✓	✗	✓
idefics-80b	80.0b	✓	✗	✓
fuyu-8b	9.4b	✓	✓	✗
Qwen-VL	9.7b	✓	✓	✓
Instruction-Tuned				
gpt-4-vision-preview	U	✗	U	✓
Bard (Gemini Update)	U	✗	U	✓
MMICL-vicuna-7b	7.9b	✓	✓	✓*
MMICL-vicuna-13b	14.2b	✓	✓	✓*
MMICL-Instructblip-T5-x1	4.0b	✓	✓	✓*
MMICL-Instructblip-T5-xxl	12.3b	✓	✓	✓*
instructblip-vicuna-7b	7.9b	✓	✓	✗
instructblip-vicuna-13b	14.2b	✓	✓	✗
instructblip-flan-t5-x1	4.0b	✓	✓	✗
instructblip-flan-t5-xxl	12.3b	✓	✓	✗
idefics-9b-instruct	8.9b	✓	✗	✓
idefics-80b-instruct	80.0b	✓	✗	✓
llava-1.5-7b-hf	7.1b	✓	✓	✗
llava-1.5-13b-hf	13.4b	✓	✓	✗
bakllava-v1-hf	7.6b	✓	U	✗
Qwen-VL-Chat	9.7b	✓	✓	✓

Table 3: Comparison of open-source and closed-source models’ attributes. **Legend:** U → Undisclosed, * → We could not utilize this feature using the official code.

held-in datasets, InstructBLIP attains state-of-the-art zero-shot performance across all 13 held-out datasets, substantially outperforming BLIP-2 and larger Flamingo models.

MMICL (Zhao et al., 2023). Unlike previous work, MMICL utilizes a novel context scheme, treating image and text representations equally and establishing the reference between image and text via image declaration. It enables users to have the flexibility to input multiple images and text in any desired order, with no restrictions on the quantity or placement of images in contexts. MMICL achieves new state-of-the-art zero-shot performance on a wide range of general vision-language tasks, especially for complex benchmarks, including MME and MMBench. Moreover, MMICL effectively tackles the challenge of complex multi-modal prompt understanding and emerges with impressive ICL ability.

GPT-4V (OpenAI, 2023). GPT-4 with vision (GPT-4V) enables users to instruct GPT-4 to analyze image inputs provided by the user and is the latest capability OpenAI is making broadly available.

Gemini (Google, 2023). The Gemini family consists of Ultra, Pro, and Nano sizes, suitable for

applications ranging from complex reasoning tasks to on-device memory-constrained use cases. Evaluation on a broad range of benchmarks shows that the Gemini Ultra model advances the state of the art in 30 of 32 of these benchmarks - notably being the first model to achieve human-expert performance on the well-studied exam benchmark MMLU and improving the state-of-the-art in every one of the 20 multi-modal benchmarks the authors examined. At the time of this publication, only the Pro version was publicly available.

C Heuristics Details.

C.1 Selecting R

Pixel. Since raw pixel values are inputs to all MLLMs in this study, we utilize the flattened pixel values as the first variation of R in our heuristics.

CLIP-ViT (Dosovitskiy et al., 2021; Radford et al., 2021). Contrasting Language-Image Pre-Training (CLIP) is adopted by most of the open-sourced MLLMs as their visual encoder. As such, we select CLIP encoding as the second variation of R in our heuristics.

C.2 Calculating α_q

We first identify all possible 2×2 submatrices in the $m \times n$ query matrix. For the horizontal axis, considering that each 2×2 pattern spans across two columns, the number of unique horizontal positions is $n - 1$. Similarly, $m - 1$ unique vertical positions are on the vertical axis. Therefore, the total number of distinct 2×2 patterns that can be extracted from an $m \times n$ matrix is $(m - 1) \times (n - 1)$. To determine the expected target representation, we first apply the formula $4 = 3 + 2 - 1$ to each submatrix; then, we average over all the calculated values. Finally, we choose the option with the smallest Euclidean distance (*i.e.*, S) to the expected target representation.

D Manual Inspection Rubric

Although puzzles and their pieces come in many shapes, colors, and orientations, solving them primarily lies in understanding the pattern in one row or column and then applying it to the one with a missing piece. We consider a generated response correct if the answer is correctly identified and the puzzle’s pattern is laid out properly within the generated reasoning. Moreover, we allow a certain degree of hallucination within the generated response

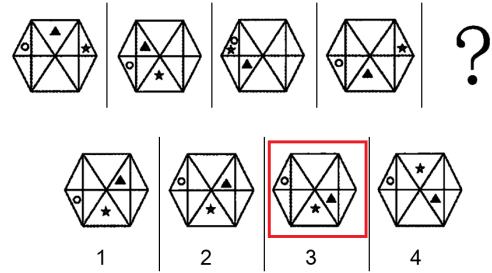


Figure 10: Example of the location pattern. Across the pieces, the triangle moves clockwise, one block at a time in the inner circle, while the five-pointed star moves clockwise, two blocks at a time in the outer circle.

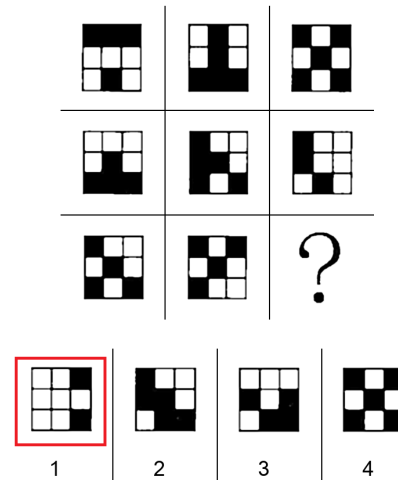


Figure 11: Example of the logic pattern. Each row follows a cell color XOR operation (0 for white and 1 for black) between the first and the second columns to make the piece in the third column.

as long as it is consistent across all shapes and does not impact the final answer. For example, if the model describes blue objects as green but correctly identifies the alternating color pattern and reasons for the desired option, we consider the reasoning correct.

E CCSE Dataset Examples

CCSE tests models’ reasoning abilities over five general patterns (*i.e.*, location, logic, progression, self-geometry, and relative-geometry) in three types of figure configurations (*i.e.*, one-row, two-rows, matrix). See Figure 10 and Figure 11 for examples.

F Prompt Examples

Table 4 and Table 5 present examples of each prompt used in our experiments.

Experiment	Prompt Example
Generalized next-token scoring	<i>[IMG]</i> You are given a puzzle. The puzzle features a set of visual patterns arranged in a matrix on the top, with the bottom right piece missing and six options at the bottom (marked by 1, 2, 3, 4, 5, or 6). Which option (either 1, 2, 3, 4, 5, or 6) fills the missing piece best?
One-by-one scoring	Here are three images: <i>[IMG1]</i> <i>[IMG2]</i> <i>[IMG3]</i> The following image is: <i>[IMG4]</i> Is it correct?
Zero-shot CoT	<i>[IMG]</i> You are given a puzzle. The puzzle features a set of visual patterns arranged in a matrix on the top, with the bottom right piece missing and six options at the bottom (marked by 1, 2, 3, 4, 5, or 6). Which option (either 1, 2, 3, 4, 5, or 6) fills the missing piece best? Let’s think step by step.
Textual reasoning	<p>Puzzle: [[yellow percentage sign, yellow percentage sign], [yellow percentage sign, ?]]</p> <p>Options: 1: yellow percentage sign 2: yellow plus sign 3: two yellow circles 4: one yellow circle 5: yellow division sign 6: yellow cross</p> <p>You are given a puzzle. The puzzle features a set of patterns arranged in a matrix on the top, with the bottom right piece missing and six options at the bottom (marked by 1, 2, 3, 4, 5, or 6). Which option (either 1, 2, 3, 4, 5, or 6) fills the missing piece best? Let’s think step by step.</p>
Visual awareness	In candidate 4 at the bottom, are the arrows arranged clockwise or counterclockwise?
Guided prompting (General)	<i>[IMG]</i> You are given a puzzle. The puzzle features a set of visual patterns arranged in a matrix on the top, with the bottom right piece missing and six options at the bottom (marked by 1, 2, 3, 4, 5, or 6). Which option (either 1, 2, 3, 4, 5, or 6) fills the missing piece best? Hint: Focus on the row-wise and column-wise changes regarding color, orientation, and shape of the puzzle pieces. Let’s think step by step.
Guided prompting (Sample-specific)	<i>[IMG]</i> You are given a puzzle. The puzzle features a set of visual patterns arranged in a matrix on the top, with the bottom right piece missing and six options at the bottom (marked by 1, 2, 3, 4, 5, or 6). Which option (either 1, 2, 3, 4, 5, or 6) fills the missing piece best? Hint: the focus should be on the column-wise changes. Let’s think step by step.
Guided prompting (Corrective)	<p>Turn 1. <i>[IMG]</i> You are given a puzzle. The puzzle features a set of visual patterns arranged in a matrix on the top, with the bottom right piece missing and six options at the bottom (marked by 1, 2, 3, 4, 5, or 6). Which option (either 1, 2, 3, 4, 5, or 6) fills the missing piece best? Let’s think step by step.</p> <p><i>[Model’s Response]</i></p> <p>Turn 2. Hint: Option 1 does not have a small circle inside it, and option 5 is a very small circle itself.</p>
Symmetrical few-shot	<p>You are given a puzzle. The puzzle features a set of visual patterns arranged in a matrix on the top, with the bottom right piece missing and six options at the bottom (marked by 1, 2, 3, 4, 5, or 6). Which option (either 1, 2, 3, 4, 5, or 6) fills the missing piece best? Let’s think step by step.</p> <p><i>[IMG1]</i> The answer is 4.</p> <p><i>[IMG2]</i> The answer is 1.</p> <p><i>[IMG3]</i></p>

Table 4: Prompt examples for our experiments. Note that all “[IMG*]” are replaced with actual images during inference.

Experiment	Prompt Example
Symmetrical few-shot CoT	<p>You are given a puzzle. The puzzle features a set of visual patterns arranged in a matrix on the top, with the bottom right piece missing and six options at the bottom (marked by 1, 2, 3, 4, 5, or 6). Which option (either 1, 2, 3, 4, 5, or 6) fills the missing piece best?</p> <p><i>[IMG1]</i></p> <p>To solve this puzzle, we need to identify a pattern or rule that applies to the rows or columns of the matrix. Let's examine the rows and columns to see if we can discern any patterns. Looking at the first row, we see a yellow percentage sign followed by a yellow percentage sign. Hence, nothing changes in the row, moving from left to right. In the second row, there's a yellow percentage sign. Following the above pattern, we deduce that the missing piece in the second row is a yellow percentage sign. Now, let's look at the columns. The first column has a yellow percentage sign, followed by a yellow percentage sign. Hence, nothing changes in the column, moving from top to bottom. The second column has a yellow percentage sign. Following the above pattern, the missing piece in the second column must be a yellow percentage sign. Combining the observations from rows and columns, we conclude that the missing piece is a yellow percentage sign.</p> <p>The provided options at the bottom are as follows:</p> <ol style="list-style-type: none"> 1. Yellow percentage sign 2. Yellow plus sign 3. Two yellow circles 4. One yellow circle 5. Yellow division sign 6. Yellow cross <p>Given these options and our conclusion, option 1 fits our criteria and best fills the missing piece.</p> <p><i>[IMG2]</i></p>
Asymmetrical few-shot CoT	<p>You are given a puzzle. The puzzle features a set of visual patterns arranged in a matrix on the top, with the bottom right piece missing and six options at the bottom (marked by 1, 2, 3, 4, 5, or 6). Which option (either 1, 2, 3, 4, 5, or 6) fills the missing piece best?</p> <p>Demonstration 1:</p> <p>Puzzle:</p> <p>[[yellow percentage sign, yellow percentage sign], [yellow percentage sign, ?]]</p> <p>Options:</p> <ol style="list-style-type: none"> 1: yellow percentage sign 2: yellow plus sign 3: two yellow circles 4: one yellow circle 5: yellow division sign 6: yellow cross <p>To solve this puzzle, we need to identify a pattern or rule that applies to the rows or columns of the matrix. Let's examine the rows and columns to see if we can discern any patterns. Looking at the first row, we see a yellow percentage sign followed by a yellow percentage sign. Hence, nothing changes in the row, moving from left to right. In the second row, there's a yellow percentage sign. Following the above pattern, we deduce that the missing piece in the second row is a yellow percentage sign. Now, let's look at the columns. The first column has a yellow percentage sign, followed by a yellow percentage sign. Hence, nothing changes in the column, moving from top to bottom. The second column has a yellow percentage sign. Following the above pattern, the missing piece in the second column must be a yellow percentage sign. Combining the observations from rows and columns, we conclude that the missing piece is a yellow percentage sign.</p> <p>The provided options at the bottom are as follows:</p> <ol style="list-style-type: none"> 1. Yellow percentage sign 2. Yellow plus sign 3. Two yellow circles 4. One yellow circle 5. Yellow division sign 6. Yellow cross <p>Given these options and our conclusion, option 1 fits our criteria and best fills the missing piece.</p> <p>Let's solve the puzzle in the image, step by step, similar to the demonstrations.</p> <p><i>[IMG]</i></p>

Table 5: Prompt examples for our experiments (Continued). Note that all “[IMG*]” are replaced with actual images during inference.